



Codimension-one and -two bifurcation analysis of a discrete-time prey-predator model

Vijay Shankar Sharma¹ · Anuraj Singh¹ · Amr Elsonbaty^{2,3} · A. A. Elsadany^{2,4}

Received: 4 January 2023 / Revised: 13 March 2023 / Accepted: 24 March 2023 / Published online: 17 April 2023
© The Author(s), under exclusive licence to Springer-Verlag GmbH Germany, part of Springer Nature 2023

Abstract

This paper investigates bifurcations analysis and resonances in a discrete-time prey-predator model analytically and numerically as well. The local stability conditions of all the fixed points in the system are determined. Here, codim-1 and codim-2 bifurcation including multiple and generic bifurcations in the discrete model are explored. The model undergoes fold bifurcation, flip bifurcation, Neimark–Sacker bifurcation and resonances 1:2, 1:3, 1:4 at different fixed points. Using the critical normal form theorem and bifurcation theory, normal form coefficients are calculated for each bifurcation. The different bifurcation curves of fixed points are drawn which validate the analytical findings. The numerical simulation gives a wide range of periodic cycles including codim-1 bifurcation and resonance curves in the system. The results in this manuscript reveal that the dynamics of the discrete-time model in both single-parameter and two-parameter spaces are inherently rich and complex. The resonance bifurcation in the discrete-time map indicates that both species coincide till order 4 in stable periodic cycles near some critical parametric values.

Keywords Fold bifurcation · Flip bifurcation · Neimark–Sacker bifurcation · Resonance bifurcation · Bifurcation curve

1 Introduction

In ecology, the interaction between distinct species causes conflict, cooperation and consumption. The prey-predator system is the most fundamental linkage among them. Almost a century ago, the predator and prey populations had many

variations based on their experimental evidence. As well as describing nonlinear ecosystem interactions such as competition, scavenging, and mutualism, the Lotka–Volterra model provides a general framework for other kinds of nonlinear interactions. The study of the dynamical behaviors of prey-predator models has drawn the attention of many mathematical ecologists [1–6].

The investigation of the prey-predator model in both cases discrete and continuous-time is a matter of interest [7–12]. For discrete-time model, the population includes non-overlapping generation i.e. population density is very low. These kinds of models are explained well by difference equation [13–16]. The discrete system can produce more realistic dynamics than the corresponding continuous counterparts [17–20]. Therefore many authors investigated discrete-time models and determined the interesting dynamical behavior including a wide range of bifurcation [21–25].

Maynard Smith [26] first studied the Lotka–Volterra discrete-time predator–prey system which was further investigated by Levine [27] and Liu and Xiao [28]. The discrete model exhibits complex dynamical behavior including flip bifurcation, fold bifurcation, and Neimark–Sacker bifurcation. In another investigation, the discrete version of the predator–prey model with Holling type-II functional

✉ A. A. Elsadany
aelsadany1@yahoo.com

Vijay Shankar Sharma
vijays@iiitm.ac.in

Anuraj Singh
anuraj@iiitm.ac.in

Amr Elsonbaty
elsonbaty2010@gmail.com

¹ ABV-Indian Institute of Information Technology and Management, Gwalior, M.P., India

² Department of Mathematics, College of Sciences and Humanities in Al-Kharj, Prince Sattam bin Abdulaziz University, Al-Kharj 11942, Saudi Arabia

³ Department of Mathematics and Engineering Physics, Faculty of Engineering, Mansoura University, Mansoura 35516, Egypt

⁴ Department of Basic Science, Faculty of Computers and Informatics, Suez Canal University, Ismailia 41522, Egypt

response was studied by Hadelar and Gerstmann [29]. Also, Li and Zhang [30] gave a detailed discussion for codimension one bifurcation and parametric restriction for stability. A discrete predator–prey model with Holling type-II functional response was investigated for bifurcation and chaotic dynamics [31]. In recent work, Singh and Deolia studied a discretized Leslie-Gower predator–prey model in which the system exhibits codimension-1 bifurcation including flip bifurcation, fold bifurcation, and Neimark–Sacker bifurcation [32]. There are several investigations in which the discrete models show interesting dynamics including bifurcation and chaos [33–38].

In the previous decade, the bifurcation for higher codimension has played a significant role in discrete-time models because it reveals more complicated dynamical behavior. Resonance bifurcations are the most crucial higher codimension bifurcation in nonlinear systems. At first Kuznetsov [39] gave the theory of codimension two resonance bifurcations. The resonance bifurcations such as 1:1(R1), 1:2(R2), 1:3(R3) and 1:4(R4) may be determined by using the critical normal form coefficient (CNFC) method. Other researchers also explored resonances bifurcation of codim-2 in the discrete-time model, see Kuznetsov and Meijer [40], Alidousti et al. [41], Eskandari and Alidousti [42, 43], Ghaziani et al. [44], Naik et al. [45, 46] etc. Eskandari and Alidousti [43] explored codim-2 bifurcation viz. generalized flip bifurcation and strong resonances in a discrete predator–prey system. Alidousti et al. [41] studied a discretized Bonhoeffer-van der Pol oscillator system and determined codim-2 bifurcation. In another study, the codimension-two resonance bifurcations is reported in Bazykin-Berezovskaya two species discrete model with Allee effect [47]. A discretized version of the two-species model with mixed functional responses was discussed by Naik et al. [48]. They resulted in a detailed bifurcation phenomenon and control of chaos.

A functional response in ecology refers to the intake rate for the predator as a function of prey density. Due to the implementation of a particular type of functional response, the dynamical behavior of the predator–prey model is affected [49]. As discussed in [50], there are generally three types of functional response in dynamical systems: linear (type-I), hyperbolic (type-II), and sigmoidal (type-III). There is a direct connection between the prey density and the predator consumption rate in the Holling type-I functional response.

Let $M(\theta)$ and $Q(\theta)$ be the prey and predator population densities, respectively. Then prey-predator model with Holling type-I functional response in prey is represented as [51]

$$\frac{dM(\theta)}{d\theta} = M(\theta)(a_1 - b_1M(\theta) - c_1Q(\theta))$$

$$\frac{dQ(\theta)}{d\theta} = Q(\theta)(c_1d_1M(\theta) - f). \tag{1}$$

The maximum per capita growth rate for prey population is represented by a_1 . The strength for intra-specific competition among prey populations is denoted by b_1 . The parameter c_1 represents the strength of intra-species competition between predator and prey. The conversion rate of prey species into predators is denoted by d_1 and the per capita death rate of predator species is described by f . All involved parameters are taken as positive.

The non-dimensionalized form of (1) can be obtained with the help of the following transformation for reducing parameters:

$$x(t) = \frac{a_1d_1M(\theta)}{f}, \quad y(t) = \frac{c_1Q(\theta)}{f} \quad \text{and} \quad t = f\theta.$$

The non-dimensionalized version of (1) is written as

$$\begin{aligned} \frac{dx(t)}{dt} &= x(t)(a - \beta x(t) - y(t)) \\ \frac{dy(t)}{dt} &= y(t)(cx(t) - 1) \end{aligned} \tag{2}$$

where $a = \frac{a_1}{f}, \beta = \frac{b_1}{a_1d_1}, c = \frac{c_1}{a_1}$.

Here we deploy a piecewise constant argument approach to discretize the model (2) [7, 23, 52]:

$$\begin{aligned} x_{n+1} &= x_n \exp(a - \beta x_n - y_n) \\ y_{n+1} &= y_n \exp(cx_n - 1). \end{aligned} \tag{3}$$

Here x_n and y_n denote prey population and predator population respectively.

The model (3) can be rewritten in form of a map

$$F : \begin{pmatrix} x \\ y \end{pmatrix} \rightarrow \begin{pmatrix} x \exp(a - \beta x - y) \\ y \exp(cx - 1) \end{pmatrix} \tag{4}$$

where all involve parameters a, β and c are positive.

Elsadany and Matouk discussed the local stability of equilibria and Neimark–Sacker bifurcation in a fractional-ordered model of (2) [51]. In another work, Lin et al. [53] studied local stability, flip bifurcation and Neimark–Sacker bifurcation in a discrete version of the model (2). The authors attempted to control the chaos by using control techniques. But as far as our knowledge, the exploration of codim-2 resonance bifurcations in the above model is missing. The most variation between our results and the studied ones is for us to investigate all codimension two resonances bifurcations including 1:2(R2), 1:3(R3) and 1:4(R4) for different parameters in the map (4). This map is a good illustration of two species interaction for non-overlapping generations.

This study obtains the normal form coefficients to confirm the nondegeneracy of codim-1 and codim-2 bifurcations in the model. The advantage of this technique is that it can avoid the conversion of the linear part of the system into Jordan form. Section 3 discusses codim-1 bifurcation such as fold bifurcation, period-doubling (flip) bifurcation and Neimark–Sacker bifurcation on varying one parameter. Section 3.2 examines various codim-2 bifurcations including 1:2 resonance(R2), 1:3 resonance(R3), and 1:4 resonance(R4) in the model when two parameters are varied. Section 4 presents a detailed numerical study using MATCONTM. Section 5 outlines a brief conclusion.

2 Fixed point and stability analysis

Let (x^*, y^*) be any fixed point of the discrete map (4) in a region $D = \{(x, y) : x, y \in \mathbb{R}_+^2\}$ such that

$$\begin{aligned} x^* \exp(a - \beta x^* - y^*) &= x^* \\ y^* \exp(cx^* - 1) &= y^*. \end{aligned}$$

The trivial fixed point $E_1^*(x_1^*, y_1^*) = (0, 0)$ always exists and two other fixed points $E_2^*(x_2^*, y_2^*)$ and $E_3^*(x_3^*, y_3^*)$ are as follows:

$$\begin{aligned} E_2^*(x_2^*, y_2^*) &= \left(\frac{a}{\beta}, 0\right), \\ E_3^*(x_3^*, y_3^*) &= \left(\frac{1}{c}, \frac{ac - \beta}{c}\right). \end{aligned}$$

The two eigenvalues are $|\Lambda_1| = |e^a| > 1$ and $|\Lambda_2| = |\frac{1}{e}| < 1$ for Jacobian matrix $J(E_1^*)$. Therefore the trivial fixed point E_1^* is a saddle point.

Similarly, the Jacobian matrix $J(E_2^*)$ gives eigenvalues $\Lambda_1 = 1 - a$ and $\Lambda_2 = e^{\frac{ac - \beta}{\beta}}$. Table 1 summarizes the local stability of semi-positive fixed point E_2^* .

Let $P(\Lambda)$ be a characteristic polynomial of associated variational matrix $J(E_3^*)$:

$$P(\Lambda) = \Lambda^2 - \text{trace}(J)\Lambda + \det(J),$$

where

$$\begin{aligned} \text{trace}(J) &= 2 - \frac{\beta}{c}, \\ \det(J) &= 1 - \frac{\beta}{c} + \frac{ac - \beta}{c}. \end{aligned}$$

Then

$$P(1) = \frac{ac - \beta}{c} > 0, \quad P(-1) = 4 - \frac{2\beta}{c} + \frac{ac - \beta}{c} > 0,$$

when $\beta < ac$.

As $P(1) > 0$ and Λ_1 and Λ_2 be two roots of characteristic equation $P(\Lambda) = 0$, we summarize the stability of fixed point E_3^* in Table 2 (from lemma 2.2 in [16]).

3 Bifurcation analysis

The map (4) can be rewritten as

$$\begin{pmatrix} x \\ y \end{pmatrix} \rightarrow F(x, y, \mu) = \begin{pmatrix} x \exp(a - \beta x - y) \\ y \exp(cx - 1) \end{pmatrix}$$

where $\mu = (a, \beta, c)$.

The corresponding Jacobian matrix J at arbitrary fixed point (x^*, y^*) is

$$J_{(x^*, y^*, \mu)} = \begin{pmatrix} (1 - \beta x^*) \exp(a - \beta x^* - y^*) & -x^* \exp(a - \beta x^* - y^*) \\ c y^* \exp(cx^* - 1) & \exp(cx^* - 1) \end{pmatrix}.$$

Let us consider a smooth map F

$$F(X) = AX + \frac{1}{2}B(X, X) + \frac{1}{6}C(X, X, X) + O(\|X\|^4)$$

where $A = J$ and B and C are multi linear functions corresponding to (4), discussed in [40].

Here

$$B(X, Y) = \begin{pmatrix} [(-2\beta + \beta^2 x)x_1 y_1 + (\beta x - 1)[x_2 y_1 + y_2 x_1] + x x_2 y_2] \exp(a - \beta x - y) \\ [c^2 y x_1 y_1 + c(x_2 y_1 + y_2 x_1)] \exp(cx - 1) \end{pmatrix},$$

$$C(X, Y, Z) = \begin{pmatrix} C_1 \\ C_2 \end{pmatrix}$$

where

$$\begin{aligned} C_1 &= [(3\beta^2 - \beta^3 x)x_1 y_1 z_1 + \beta(2 - \beta x)[x_2 y_1 z_1 + x_1 y_1 z_2 + x_1 y_2 z_1] \\ &\quad + (1 - \beta x)[x_2 y_1 z_2 + x_2 y_2 z_1 + x_1 y_2 z_2] - x x_2 y_2 z_2] \exp(a - \beta x - y), \\ C_2 &= [(c^3 y)x_1 y_1 z_1 + c^2[x_2 y_1 z_1 + x_1 y_1 z_2 + x_1 y_2 z_1]] \exp(cx - 1) \end{aligned}$$

and $X = (x_1, x_2)^T, Y = (y_1, y_2)^T, Z = (z_1, z_2)^T$.

Table 1 Properties of semi-positive fixed point $E_2^*(\frac{a}{\beta}, 0)$

Conditions		Eigenvalues		Properties
		$\Lambda_1 = 1 - a$	$\Lambda_2 = e^{\frac{ac - \beta}{\beta}}$	
$0 < a < 2$	$\beta < ac$	$ \Lambda_1 < 1$	$\Lambda_2 < 1$	Sink
	$\beta > ac$		$\Lambda_2 > 1$	Saddle
	$\beta = ac$		$\Lambda_2 = 1$	Non-hyperbolic
$a = 2$	$\beta > ac$	$ \Lambda_1 = 1$	$\Lambda_2 < 1$	Non-hyperbolic
	$\beta > ac$		$\Lambda_2 > 1$	Non-hyperbolic
	$\beta = ac$		$\Lambda_2 = 1$	Non-hyperbolic
$a > 2$	$\beta > ac$	$ \Lambda_1 > 1$	$\Lambda_2 > 1$	Saddle
	$\beta < ac$		$\Lambda_2 < 1$	Unstable
	$\beta = ac$		$\Lambda_2 = 1$	Non-hyperbolic

Table 2 Properties of a positive fixed point $E_3^*(\frac{1}{c}, \frac{ac - \beta}{c})$

Conditions	Eigenvalues	Properties
$0 < a \leq 2$	$\frac{\beta}{a} < c < \frac{2\beta}{a}$	$ \Lambda_{1,2} < 1$
$2 < a < 8$	$\frac{3\beta}{4+a} < c < \frac{2\beta}{a}$	$ \Lambda_{1,2} < 1$
$a > 2$	$\frac{\beta}{a} < c < \frac{3\beta}{4+a}$	$ \Lambda_1 < 1, \Lambda_2 > 1$ or $ \Lambda_1 > 1, \Lambda_2 < 1$
$0 < a \leq 8$ or $a > 8$	$c > \frac{3\beta}{4+a}$ or $c > \frac{2\beta}{a}$	$ \Lambda_{1,2} > 1$
$a \neq 8, a > 2$	$c = \frac{3\beta}{4+a}$	$\Lambda_1 = -1, \Lambda_2 \neq \pm 1$
$0 < a < 8$	$c = \frac{2\beta}{a}$	$ \Lambda_{1,2} = 1$

3.1 Codimension-1 bifurcations at semi-positive fixed point (E_2^*)

In this section, fold bifurcation and degenerate flip bifurcation are being determined at fixed point E_2^* .

3.1.1 Fold bifurcation

Theorem 1 *There is an occurrence of non-degenerate fold bifurcation in the system (4) at $E_2^*(x_2^*, y_2^*)$ when*

- (i) $\beta = ac$, provided $a \neq 0, 2$.
- (ii) $a = \frac{\beta}{c}$, provided $a \neq 0, 2$.
- (iii) $c = \frac{c\beta}{a}$, provided $a \neq 0, 2$.

Proof (i) From Table 2, it can be noted that the associated Jacobian matrix $J(E_2^*)$ has one eigenvalue $\Lambda_1 = 1$ and other eigenvalue $\Lambda_2 \neq \pm 1$ when $\beta = ac$ and $a \neq 0, 2$.

The center manifold at $\beta = ac$ is taken as

$$M_{LP}(v) \rightarrow qv + m_2v^2 + O(v^3),$$

$$M : \mathbb{R} \rightarrow \mathbb{R}^2, \quad m_2 = (m_{21}, m_{22})^T \tag{5}$$

where

$$Jv = v, \quad J^T u = u, \quad \langle u, v \rangle = 1$$

and

$$v = \begin{pmatrix} -1 \\ ac \\ 1 \end{pmatrix}, \quad u = \begin{pmatrix} 0 \\ 1 \end{pmatrix}.$$

The restriction of the map (4) on (5) has the following form:

$$v \rightarrow H(v) = v + \frac{1}{2}\hat{a}v^2 + O(v^3). \tag{6}$$

For center manifold invariance, it is obtained

$$F(M_{LP}(v, \mu^*)) = M(H(v, \mu^*)), \tag{7}$$

where $\mu^* = (a, ac, \beta)^T$.

Now we calculate the required condition

$$(J - I_2)m_2 = 2\hat{a} - B(v, u, \mu^*). \tag{8}$$

We apply solvability conditions to the singular system (8), it is obtained

$$\langle u, 2\hat{a} - B(v, v, \mu^*) \rangle = 0,$$

then

$$\hat{a} = \frac{1}{a}.$$

Thus fold bifurcation occurs in the map (6) at E_2^* .

The critical normal form coefficients (CNFCs) of fold bifurcation, given in theorem 1, are determined as

- (i) when $\beta = ac \Rightarrow \hat{a} = \frac{1}{a}$, provided $a \neq 0, 2$,
- (ii) when $a = \frac{\beta}{c} \Rightarrow \hat{a} = \frac{c}{\beta}$, provided $a \neq 0, 2$,
- (iii) when $c = \frac{\beta}{a} \Rightarrow \hat{a} = \frac{1}{a}$, provided $a \neq 0, 2$.

A fold bifurcation implies that a fixed point can never be destroyed and must exist for all values of a parameter. In such case, as the parameter changes, the fixed point may lose its stability. \square

3.1.2 Period doubling (flip) bifurcation

Theorem 2 A non-degenerate flip (Period-doubling) bifurcation occurs in the system (4)

- (i) at $E_2^*(x_2^*, y_2^*)$ for $a = 2$ when $\beta \neq 2c$,
- (ii) at $E_3^*(x_3^*, y_3^*)$ for $c = \frac{3\beta}{4+a}$ when $a \neq 2, 8$.

Proof (i) From Table 1, it can be observed that corresponding Jacobian matrix $J(E_2^*)$ has eigenvalue $\Lambda_1 = -1$ and $\Lambda_2 \neq \pm 1$, for $\beta \neq 2c$.

The centre manifold for the map (4) at $a = 2$ is

$$\begin{aligned} M_{PD}(v) &\rightarrow qv + m_2v^2 + m_3v^3 + O(v^4), \\ M : \mathbb{R} &\rightarrow \mathbb{R}^2, \quad m_2 = (m_{21}, m_{22})^T. \end{aligned} \tag{9}$$

The eigenvectors corresponding to eigenvalue -1 such that

$$Jv = -v, \quad J^T u = -u, \quad \langle u, v \rangle = 1$$

$$\text{where } v = \begin{pmatrix} 1 \\ 0 \end{pmatrix}, \quad u = \begin{pmatrix} 1 \\ \frac{2}{\beta \left(1 + e^{\left(\frac{2c - \beta}{\beta} \right)} \right)} \end{pmatrix}.$$

The map (4) can be written in the normal form at critical parameter

$$v \rightarrow H(v) = -v + b_{PD}v^3 + O(v^4). \tag{10}$$

The invariance in the center manifold gives

$$F(M_{PD}(v, \mu^*)) = M(H(v, \mu^*)). \tag{11}$$

Now we collect the power of v up to third order in the above expansion, we get

$$(J - I_2)m_2 = -B(v, v, \mu^*), \tag{12}$$

$$(J + I_2)m_3 = 6b_{PD}v - C(v, v, v, \mu^*) - 3B(v, m_2, \mu^*) \tag{13}$$

where $\mu^* = (a, \beta, c) = (2, \beta, c)$.

If the system (12) is non-singular, $m_2 = \begin{pmatrix} 0 \\ 0 \end{pmatrix}$.

The solvability conditions of (13) yields

$$\langle u, 6b_{PD}v - C(v, v, v, \mu^*) - 3B(v, m_2, \mu^*) \rangle = 0.$$

We get

$$b_{PD} = \frac{\beta^2}{6}.$$

The period-doubling bifurcation is non-degenerate provided $b_{PD} \neq 0$.

For $b_{PD} > 0$, bifurcation is super-critical otherwise sub-critical bifurcation for $b_{PD} < 0$.

(ii) The proof is similar line to the theorem 2(i).

The CNFC for period-doubling bifurcation is obtained as

$$b_{PD} = \frac{32 - 2a^3(-1 + \beta) + 67\beta + 3(-8 + 5\beta)}{2\beta(a - 8)(a - 2)^2}.$$

The period-doubling bifurcation is non-degenerate if $b_{PD} \neq 0$. The double period cycle is stable and hence super-critical bifurcation occurs for $b_{PD} > 0$. For $b_{PD} < 0$, the period-2 cycle is unstable i.e. sub-critical bifurcation occurs. \square

3.1.3 Neimark–Sacker bifurcation

Theorem 3 The map (4) exhibits non-degenerate Neimark–Sacker bifurcation (NSB) at fixed point E_3^* for $c = \frac{2\beta}{a}$, provided $a \neq 0, 8$ and $\beta < 4c$.

Proof It is evident from Table 2, for non-hyperbolicity of fixed point E_3^* , $c = \frac{2\beta}{a}$; $a \neq 0, 8$ and $\beta < 4c$. And $J(E_3^*)$ have complex conjugate eigenvalues with unit modulus i.e. $|\Lambda_{1,2}| = 1$.

The eigenvalues of the Variation matrix J are $\Lambda_{1,2} = \alpha_1 \pm i\alpha_2$ where $\alpha_1 = \frac{4-a}{4}$ and $\alpha_2 = \frac{1}{4}\sqrt{(8-a)a}$.

The non-degeneracy condition $\Lambda_{1,2}^j \neq 0$ ($j = 1, 2, 3, 4$) are satisfied.

For the map (4), at critical parameter value $c = \frac{2\beta}{a}$ then the center manifold form is taken as

$$M_{NS}(v, \bar{v}) = qv + \bar{v}\bar{q} + \sum_{2 \leq r+s} \frac{1}{(r+s)!} m_{rs} v^r v^{-s}, \quad v, m_{rs} \in \mathbb{C}. \quad (14)$$

And corresponding to both eigenvalues the eigenvectors are as follows

$$Jv = e^{i\theta_0}v, \quad J^T u = e^{-i\theta_0}u, \quad \langle u, v \rangle = 1.$$

The map (4) is restricted to (14) at value c

$$v \rightarrow H_{NS} = e^{i\theta_0}v + d_{NS}v|v|^2 + O(v^4), \quad v \in \mathbb{C} \quad (15)$$

where d_{NS} is a complex number.

The invariance in manifold gives

$$F(M_{NS}(v, \mu^*)) = M(H_{NS}(v, \mu^*)). \quad (16)$$

On collecting the power of v up to third order in (16), it is obtained

$$(J - e^{2i\theta_0}I_2)m_{20} = -B(v, v, \mu^*), \quad (17)$$

$$(J - I_2)m_{11} = -B(v, \bar{v}, \mu^*), \quad (18)$$

$$(J - e^{3i\theta_0}I_2)m_{30} = -C(v, v, v, \mu^*) - 3B(v, m_{20}, \mu^*), \quad (19)$$

$$(J - e^{i\theta_0}I_2)m_{21} = 2d_{NS}v - C(v, v, \bar{v}, \mu^*) - B(\bar{v}, m_{20}, \mu^*) - 2B(v, m_{11}, \mu^*) \quad (20)$$

where $\mu^* = \left(a, \beta, \frac{2\beta}{a}\right)$.

For reducing the complexity in computation, we consider $a = 3.5$, $\beta = 4.8$ and c as a free parameter. The matrix $J(E_3^*)$ gives eigenvalues

$$\Lambda_{1,2} = 0.125001 \pm 0.992158i.$$

As the systems (17)-(19) are non-singular, they have a unique solution.

The solutions of systems can be easily obtained as

$$\begin{aligned} m_{20} &= -(J - e^{2i\theta_0}I_2)^{-1}B(v, v, \mu^*) \\ &\Rightarrow m_{20} = \begin{pmatrix} -0.038095007 - 0.418205240i \\ -0.588668474 + 0.8734819542i \end{pmatrix}, \\ m_{11} &= -(A - I_2)^{-1}B(v, \bar{v}, \mu^*) \\ &\Rightarrow m_{11} = \begin{pmatrix} 0 \\ 0 \end{pmatrix}. \end{aligned}$$

Since the system (20) is singular, we use Fredholm's solvability condition

$$\langle u, 2d_{NS}v - C(v, v, \bar{v}, \mu^*) - B(\bar{v}, m_{20}, \mu^*) - 2B(v, m_{11}, \mu^*) \rangle = 0.$$

The value of d_{NS} is calculated as

$$d_{NS} = 1.46954 - 0.653601i.$$

For Neimark–Sacker bifurcation the first Lyapunov coefficient gives

$$c_{NS} = R(e^{-i\theta_0}d_{NS}) = -0.464781491 < 0.$$

In the above calculation the value of u, v are taken as

$$\begin{aligned} v &= \begin{pmatrix} -0.182292 - 0.206704i \\ 1 \end{pmatrix}, \\ u &= \begin{pmatrix} 0.1179235213 + 2.346524261i \\ 0.500925484 + 0.44165478i \end{pmatrix}. \end{aligned}$$

Since $c_{NS} < 0$, the Neimark–Sacker bifurcation (NSB) is super-critical and a closed invariant curve appears which is stable i.e. both species can fluctuate near critical parameter values and the stable oscillations may appear. \square

3.2 Codimension-2 bifurcation analysis

This subsection illustrates codim-2 bifurcation analysis along with strong resonances R2(1:2), R3(1:3) and R4(1:4).

3.2.1 1:2 resonance at E_3^*

Theorem 4 The map (4) exhibits 1:2 resonance bifurcation at fixed point E_3^* for $a = 8$ and $c = \frac{\beta}{4}$.

Proof At the fixed point E_3^* , the corresponding $J(E_3^*)$ has two multipliers $\Lambda_{1,2} = -1$ when $\text{trace}(J(E_3^*)) = -2$, $\text{Det}(J(E_3^*)) = 1$. It implies that $a = 8$, $c = \frac{\beta}{4}$.

Here we consider the center manifold form of the map (4)

$$M_{R2}(v_1, v_2) = q_0v_1 + v_2q_1$$

$$+ \sum_{2 \leq r+s \leq 3} \frac{1}{r!s!} m_{rs} v_1^r v_2^s, \quad v, m_{rs} \in C. \tag{21}$$

The eigenvectors corresponding to both eigenvalues are

$$Jq_0 = -q_0, \quad Jq_1 = -q_1 + q_0, \\ J^T p_0 = -p_0, \quad J^T p_1 = -p_1 + p_0,$$

and

$$\langle p_0, q_1 \rangle = \langle p_1, q_0 \rangle = 1, \quad \langle p_0, q_0 \rangle = \langle p_1, q_1 \rangle = 0.$$

where

$$q_0 = \begin{pmatrix} 1 \\ -\beta \\ -2 \end{pmatrix}, \quad q_1 = \begin{pmatrix} 1 \\ \frac{2}{\beta} \\ 0 \end{pmatrix}, \\ p_0 = \begin{pmatrix} -2 \\ -4 \\ \beta \end{pmatrix}, \quad p_1 = \begin{pmatrix} 0 \\ -2 \\ \beta \end{pmatrix}.$$

The map (4) can be restricted as follows:

$$\begin{pmatrix} v_1 \\ v_2 \end{pmatrix} \rightarrow H_{R2}(v) = \begin{pmatrix} -v_1 + v_2 \\ -v_2 + C_{R2}v_1^3 + D_{R2}v_1^2v_2 \end{pmatrix}, \\ v = (v_1, v_2) \in C. \tag{22}$$

The invariance condition of the central manifold gives

$$F(M_{R2}(v, \mu^*)) = M_{R2}(H_{R2}(v, \mu^*)). \tag{23}$$

On collecting power of v up to third order in above expansion (23), we get

$$(J - I_2)m_{20} = -B(q_0, q_0, \mu^*) \\ \Rightarrow m_{20} = \begin{pmatrix} 0 \\ 0 \end{pmatrix}, \tag{24}$$

$$(J - I_2)m_{11} = -B(q_0, q_1, \mu^*) - m_{20}, \\ \Rightarrow m_{11} = \begin{pmatrix} \frac{\beta}{16} \\ -\frac{\beta^2}{8} \end{pmatrix}, \tag{25}$$

$$(J - I_2)m_{02} = -B(q_1, q_1, \mu^*) - 2m_{11} + m_{20} \\ \Rightarrow m_{02} = \begin{pmatrix} \frac{-3c}{4} \\ \frac{9\beta^2}{8} \end{pmatrix}. \tag{26}$$

The cubic terms of (23) yields

$$(J + I_2)m_{30} = 6C_{R2}q_1 + C(q_0, q_0, q_0, \mu^*)$$

$$-3B(q_0, m_{20}, \mu^*), \tag{27}$$

$$(J + I_2)m_{21} = 2D_{R2}q_1 - C(q_0, q_0, q_1, \mu^*) \\ -2B(q_0, m_{11}, \mu^*) \\ -B(q_1, m_{20}, \mu^*) + m_{30} \tag{28}$$

$$(J + I_2)m_{12} = -C(q_0, q_0, q_0, \mu^*) - 2B(q_1, m_{11}, \mu^*) \\ -B(q_0, m_{02}, \mu^*) \\ -m_{30} + 2m_{21} \tag{29}$$

$$(J + I_2)m_{03} = -C(q_1, q_1, q_1, \mu^*) \\ -3B(q_1, m_{02}, \mu^*) + 3(m_{12} - m_{21}) \\ + m_{30} \tag{30}$$

where $\mu^* = \left(a = 8, \beta, \frac{\beta}{4} \right)$.

The solvability condition for the singular system (27) is

$$\langle p_0, 6C_{R2}q_1 + C(q_0, q_0, q_0, \mu^*) - 3B(q_0, m_{20}, \mu^*) \rangle = 0$$

we get

$$C_{R2} = \frac{19\beta + 14\beta^2}{48}.$$

The singular system (28) has a unique solution if

$$\langle p_0, 2D_{R2}q_1 - C(q_0, q_0, q_1, \mu^*) - 2B(q_0, m_{11}, \mu^*) \\ -B(q_1, m_{20}, \mu^*) + m_{30} \rangle = 0$$

since

$$\langle p_0, m_{30} \rangle = -\langle p_1, 3B(q_0, m_{20}, \mu^*) + C(q_0, q_0, q_0, \mu^*) \rangle \\ = \frac{-5\beta}{8}.$$

The third-order coefficient can be calculated as

$$D_{R2} = \frac{36\beta - 19\beta^2}{64}.$$

The non-degeneracy conditions of 1:2 resonance bifurcation $C_1 = 4C_{R2} \neq 0$ and $D_1 = -2D_{R2} - 6C_{R2} \neq 0$ are satisfied. The sign of C_1 indicates the behavior of a fixed point. If $C_1 < 0$ then there is occurred Niemark-Sacker bifurcation curve and if $C_1 > 0$ then bifurcation is supercritical. The 1:2 resonance bifurcation scenario is determined by the coefficient D_1 . \square

3.2.2 1:3 resonance at E_3^*

Theorem 5 *The system (4) undergoes non-degenerate 1:3 resonance bifurcation at fixed point E_3^* when $a = 6$ and $c = \frac{\beta}{3}$.*

Proof The eigenvalues of Jacobian matrix $J(E_3^*)$ are in form of complex conjugate $e^{\pm \frac{2\pi i}{3}}$ when $trace(J(E_3^*)) = 1$ and $Det(J(E_3^*)) = 1$ with $a = 6, c = \frac{\beta}{3}$.

Now we consider the center manifold form of a map (4) as

$$M_{R3}(v, \bar{v}) = qv + \bar{v}\bar{q} + \sum_{2 \leq r+s} \frac{1}{(r+s)!} m_{rs} v^r v^{-s}, \quad v, m_{rs} \in C. \tag{31}$$

The eigenvectors corresponding to both eigenvalues are

$$Jq = e^{\frac{2\pi i}{3}} q, \quad J^T p = e^{-\frac{2\pi i}{3}} p, \quad \langle p, q \rangle = 1$$

$$\text{where } q = \begin{pmatrix} -\frac{3+i\sqrt{3}}{2\beta} \\ 1 \end{pmatrix}, \quad p = \begin{pmatrix} \frac{i\beta\sqrt{3}}{6} \\ \frac{1+i\sqrt{3}}{2} \end{pmatrix}.$$

The map (4) is restricted to the form

$$v \rightarrow H_{R3}(v) = e^{i\frac{2\pi}{3}} v + B_{R3} \bar{v}^2 + C_{R3} v|v|^2 + O(v^4), \quad v \in C. \tag{32}$$

The center manifold invariance property requires

$$F(M_{R3}(v, \mu^*)) = M_{R3}(H_{R3}(v, \mu^*)). \tag{33}$$

We collect quadratic terms of (33) in above expansion, it is obtained

$$(J - e^{\frac{4\pi i}{3}} I_2) m_{20} = 2B_{R3} \bar{q} - B(q, q, \mu^*), \tag{34}$$

$$(J - I_2) m_{11} = -B(q, \bar{q}, \mu^*), \tag{35}$$

$$(J - e^{-\frac{4\pi i}{3}} I_2) m_{02} = 2B_{R3} q - B(\bar{q}, \bar{q}, \mu^*), \tag{36}$$

where $\mu^* = (a = 6, \beta, c = \frac{\beta}{3})$.

On using the Fredholm condition to the singular system (37), we get

$$\langle p, 2B_{R3} q - B(\bar{q}, \bar{q}, \mu^*) \rangle = 0 \Rightarrow B_{R3} = \frac{-3 - 5\sqrt{3}i}{12}$$

and

$$\bar{B}_{R3} = \frac{-3 + 5\sqrt{3}i}{12}.$$

Now we collect $v^2 \bar{v}$ -terms in (33) which gives

$$(J - e^{\frac{2\pi i}{3}} I_2) m_{21} = 2c_{R3} q + e^{-\frac{2\pi i}{3}} \bar{B}_{R3} m_{02} - 2B(q, m_{11}, \mu^*) - B(\bar{q}, m_{20}, \mu^*) - C(q, q, \bar{q}, \mu^*). \tag{37}$$

As the system (37) is singular, it can be solved if

$$\begin{aligned} \langle p, 2c_{R3} q + e^{-\frac{2\pi i}{3}} \bar{B}_{R3} m_{02} - 2B(q, m_{11}, \mu^*) \\ - B(\bar{q}, m_{20}, \mu^*) \\ - C(q, q, \bar{q}, \mu^*) \rangle = 0. \end{aligned} \tag{38}$$

We get

$$C_{R3} = \frac{27 - 15\beta + (43\beta - 45)\sqrt{3}i}{36\beta}.$$

The dynamical behavior of the invariant closed curve is determined by

$$L = Re \left(\frac{1}{3} \left(\frac{e^{\frac{4\pi i}{3}} C_{R3}}{|B_{R3}|} - 1 \right) \right).$$

For $|B_{R3}| \neq 0$ as well as, $L \neq 0$ the 1:3 resonance bifurcation indicates that an invariant curve of period three is bifurcated from the fixed point near R3 point. \square

3.2.3 1:4 resonance at E_3^*

Theorem 6 The map (4) shows non-degenerate 1:4 resonance bifurcation at fixed point E_3^* when $a = 4$ and $c = \frac{\beta}{2}$.

Proof For 1:4 resonance bifurcation, there is an eigenvalue in a pair of complex conjugate $e^{\pm \frac{\pi i}{2}}$ in corresponding Jacobian matrix $J(E_3^*)$ when

$$\begin{aligned} trace(J(E_3^*)) = 0 \quad \text{and} \quad Det(J(E_3^*)) = 1 \\ \text{i.e. } a = 4 \quad \text{and} \quad c = \frac{\beta}{2}. \end{aligned}$$

Now we consider the center manifold form of map (4)

$$M_{R4}(\zeta, \bar{\zeta}) = q\zeta + \bar{\zeta}\bar{q} + \sum_{2 \leq r+s} \frac{1}{(r+s)!} m_{rs} \zeta^r \zeta^{-s}, \quad \zeta, m_{rs} \in C. \tag{39}$$

The eigenvectors corresponding to both eigenvalues give

$$Jq = e^{\frac{\pi i}{2}} q, \quad J^T p = e^{-\frac{\pi i}{2}} p, \quad \langle p, q \rangle = 1,$$

where

$$q = \begin{pmatrix} -\frac{1+i}{\beta} \\ 1 \end{pmatrix}, \quad p = \begin{pmatrix} \frac{(1+i)\beta}{2} \\ 1 \end{pmatrix}.$$

We normalize the vector p with respect to q as

$$p = \begin{pmatrix} \frac{i\beta}{2} \\ \frac{1+i}{2} \end{pmatrix}.$$

The restriction of the map (4) on (39) at parameters c and a is

$$\zeta \rightarrow H_{R4}(\zeta) = i\zeta + C_{R4}\zeta^2\bar{\zeta} + D_{R4}\zeta^3 + O(\zeta^4), \quad \nu \in C. \tag{40}$$

The invariance condition in the center manifold yields

$$F(M_{R4}(\zeta, \mu^*)) = M_{R4}(H_{R4}(\zeta, \mu^*)). \tag{41}$$

With the above expansion (41), we can determine ζ 's power up to the second order

$$(J + I_2)m_{20} = -B(q, q, \mu^*) \Rightarrow m_{20} = \begin{pmatrix} \frac{1+2i}{\beta} \\ -1 \end{pmatrix}, \tag{42}$$

$$(J - I_2)m_{11} = -B(q, \bar{q}, \mu^*) \Rightarrow m_{11} = \begin{pmatrix} 0 \\ 0 \end{pmatrix}, \tag{43}$$

$$(J + I_2)m_{02} = -B(\bar{q}, \bar{q}, \mu^*) \Rightarrow m_{02} = \begin{pmatrix} 1+2i \\ -i \end{pmatrix} \tag{44}$$

where $\mu^* = (a = 4, \beta, c = \frac{\beta}{2})$.

For getting resonance terms in (41)

$$(J - e^{\frac{\pi}{2}i} I_2)m_{21} = 2C_{R4}q - C(q, q, \bar{q}, \mu^*) - 2B(q, m_{11}, \mu^*) - B(\bar{q}, m_{20}, \mu^*), \tag{45}$$

$$(J - e^{\frac{\pi}{2}i} I_2)m_{03} = 6D_{R4}q - C(\bar{q}, \bar{q}, \bar{q}, \mu^*) - 3B(\bar{q}, m_{02}, \mu^*). \tag{46}$$

The Fredholm solvability conditions of the singular system (45) and (46) give

$$\begin{aligned} \langle p, 2C_{R4}q - C(q, q, \bar{q}, \mu^*) - 2B(q, m_{11}, \mu^*) - B(\bar{q}, m_{20}, \mu^*) \rangle &= 0, \\ \langle p, 6D_{R4}q - C(\bar{q}, \bar{q}, \bar{q}, \mu^*) - 3B(\bar{q}, m_{02}, \mu^*) \rangle &= 0. \end{aligned}$$

We have

$$C_{R4} = \frac{3i}{8},$$

$$D_{R4} = \frac{(11 - 15\beta) + (16 - 3\beta)i}{24}.$$

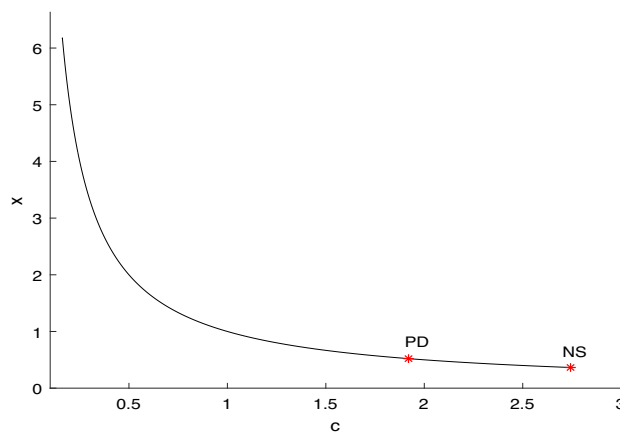


Fig. 1 Bifurcation curve with respect to c

The 1:4 resonance bifurcation curve is determined by

$$A_0 = \frac{-iC_{R4}}{|D_{R4}|}.$$

The coefficient A_0 determines the bifurcation scenario near R4 resonance point on the curve for $|D_{R4}| \neq 0$. The 1:4 resonance bifurcation demonstrates that both species coexist till order 4 in stable periodic cycles near some critical parametric values. □

4 Numerical computation

To validate our analytic findings, we use the MATLAB package MATCONTM to demonstrate the dynamical behavior of the map (4) [54, 55].

4.1 Numerical continuation of $E_3^*(x^*_3, y^*_3)$

We compute the fixed point E_3^* . We consider $a = 3.5, \beta = 4.8$, and vary c as a bifurcation parameter. MATCONTM generates the following report:

```
For NS, x=(0.364583 1.750000 2.742856)
normal form coefficient (NFC) of NS =
-4.647035e-01
For PD, x=(0.520833 1.000000 1.920000)
NFC of PD=1.598668e+00.
```

From theorem 2, the map (4) demonstrates a period-doubling bifurcation at positive fixed point E_3^* . By theorem 3, the map (4) shows Neimarck–Sacker bifurcation at E_3^* when critical parameter $c = 2.742856$. The period-doubling point and Neimarck–Sacker point are detected in the MATCONTM report by PD and NS respectively, shown in Fig. 1. Figure 2 shows the 3-dimensional bifurcation diagram of Neimarck–Sacker and Period-doubling bifurcations together and associated maximum Lyapunov exponents (MLE) at

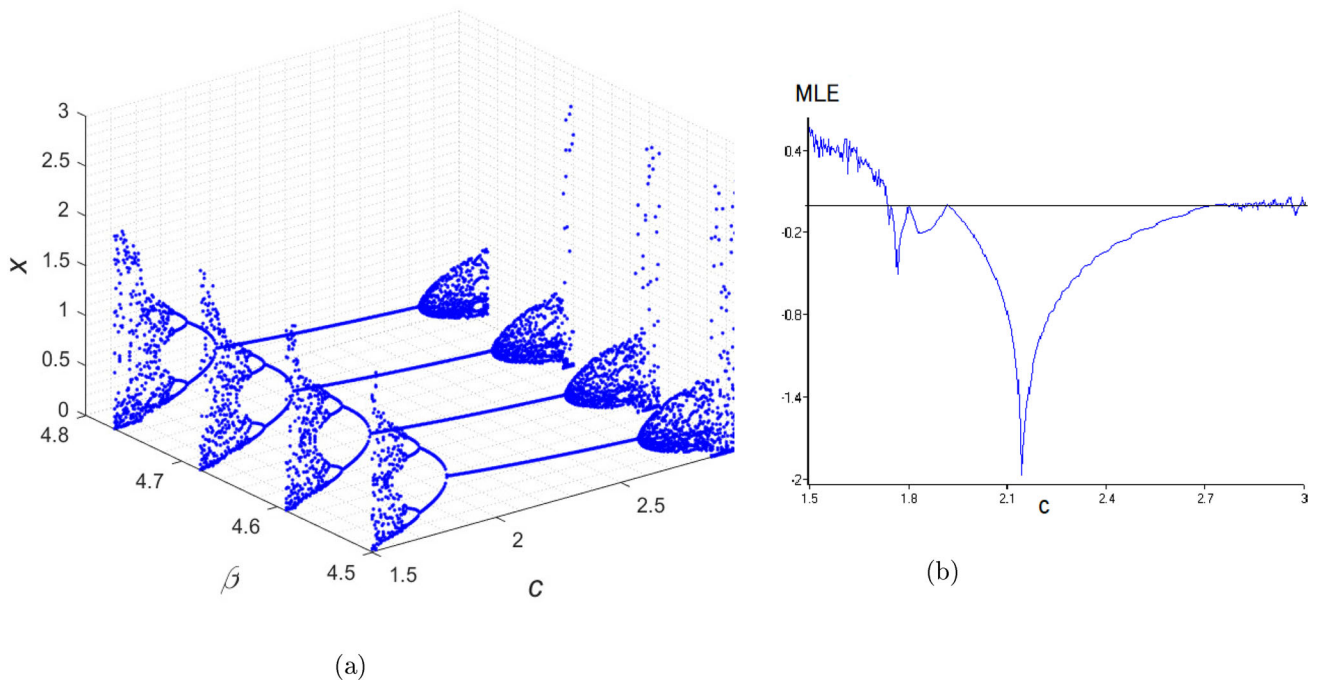


Fig. 2 3D bifurcation diagram for both Neimark–Sacker and period-doubling and associated MLE

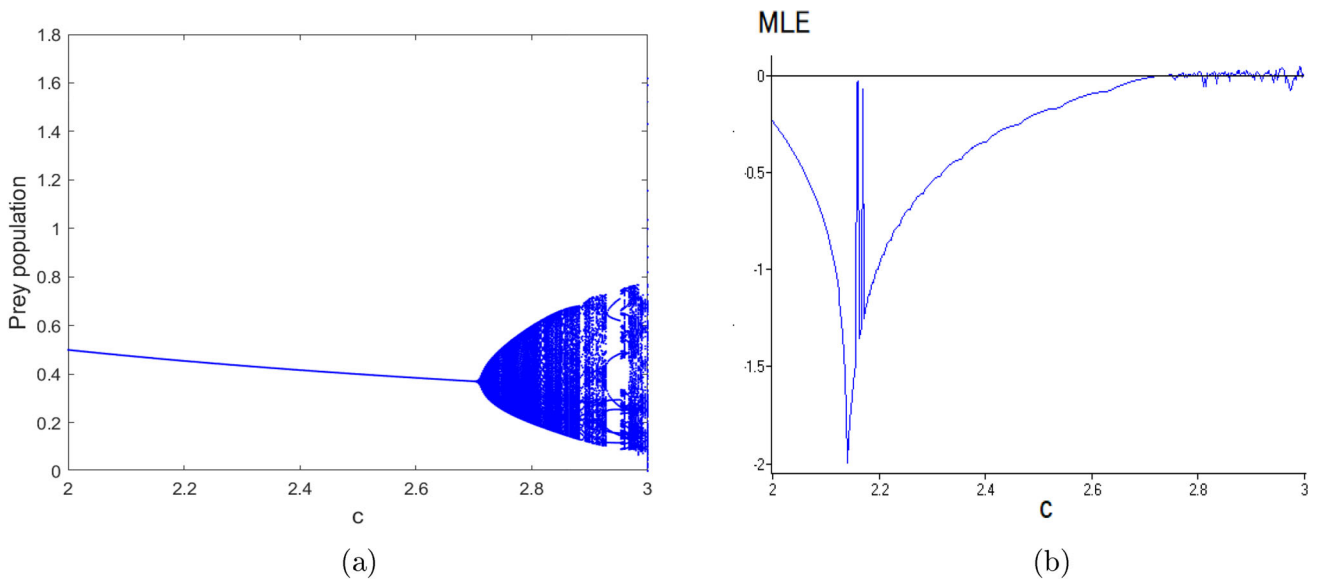


Fig. 3 The Neimark–Sacker bifurcation diagram and associated MLE

$a = 3.5$, corresponding to Fig. 1. A Neimark–Sacker bifurcation diagram with respect to c and associated maximum Lyapunov exponents (MLE) is also drawn in Fig. 3 at $a = 3.5$ and $\beta = 4.8$.

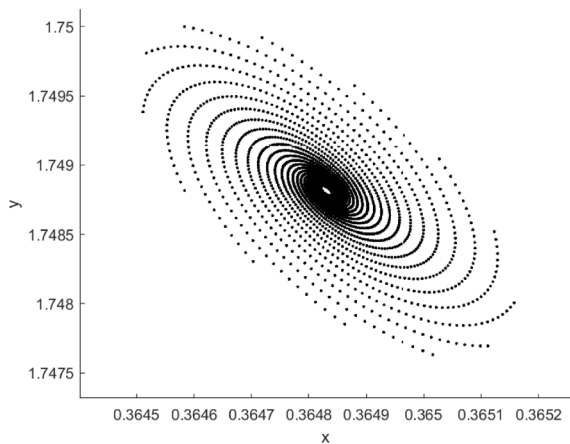
The phase plot diagrams are drawn in Fig. 4 for different values of c corresponding to near NS point, pointed in Fig. 1. If the value $c = 2.741$ then the fixed point E_3^* is a stable attractor, depicted in Fig. 4a. A closed invariant curve occurs at $c = 2.7428$ in Fig. 4b. After NS point the behavior of the

system (4) is drawn in Fig. 4c at $c = 2.751$. Figure 4d shows the breakdown of a closed curve at $c = 2.9$. At $c = 3.0$, a fractal structure appears in Fig. 4e.

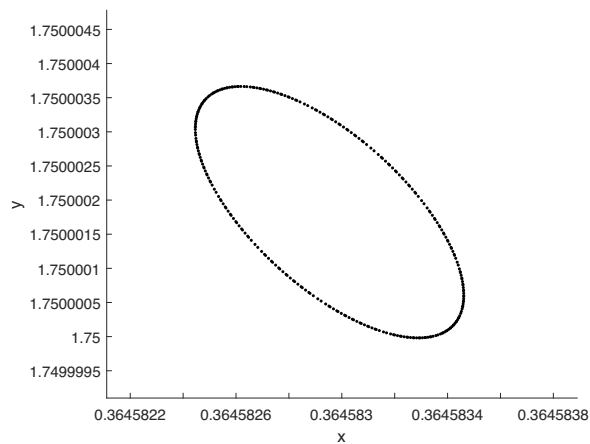
Now, we select the PD point in Fig. 1. The MATCONTM gives expression as follows

The statements of MATCONTM for a continuation of 2-cycles are

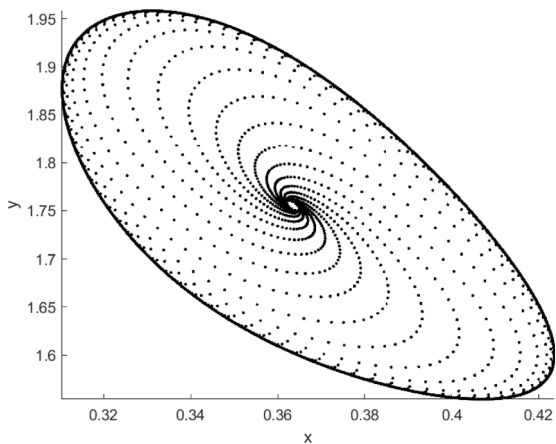
```
For PD, x=(0.245707 1.062659 1.801556)
NFC of PD=1.768882e+01
```



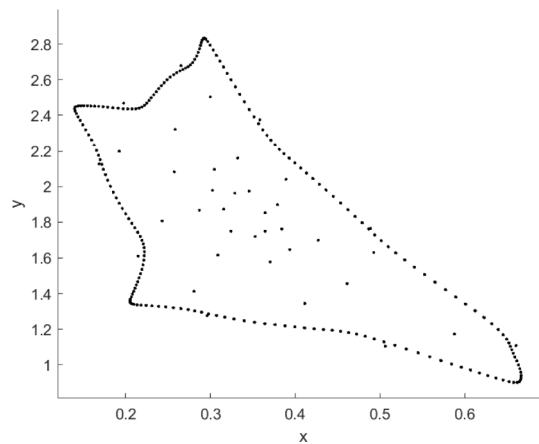
(a) for $c = 2.741$



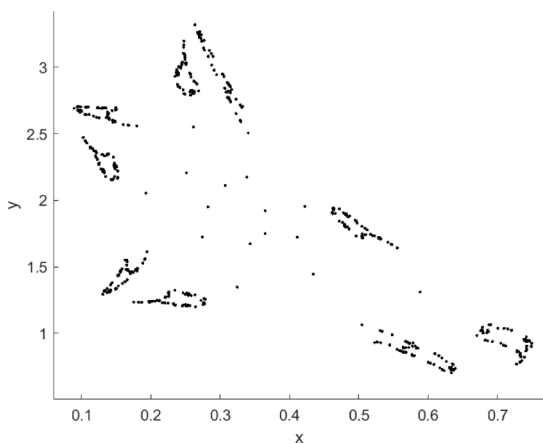
(b) for $c = 2.74286$



(c) for $c = 2.751$



(d) for $c = 2.9$



(e) for 3.0

Fig. 4 Phase plots of map (4) corresponding to NS point in Fig (1). **a** Attractor before NSB for $c = 2.741$. **b** Neimarc–Sacker bifurcation for $c = 2.74286$. **c** Closed invariant curve for $c = 2.751$. **d** Breakdown of closed invariant curve for $c = 2.9$. **e** Chaotic attractor for $c = 3.01$

For PD, $x=(0.864445 \ 0.608614 \ 1.801556)$
 NFC of PD= $7.057426e+01$.

The continuation of 4-cycle at E_3^* in fourth iterations:

For PD, $x = (0.805153 \ 0.545971 \ 1.748160)$
 NFC of PD = $3.512630e+02$
 For PD, $x = (0.997368 \ 0.531802 \ 1.748160)$
 NFC of PD = $9.141226e+02$
 label for PD, $x = (0.1617341 \ 1.118596 \ 1.748160)$
 NFC of PD = $4.9081175e+02$
 label for PD, $x = (0.323865 \ 0.8206555 \ 1.748160)$
 NFC PD = $1.140418e+02$.

A cascade of 2-cycles and 4-cycles period doubling curves are drawn in Fig. 5. The corresponding bifurcation diagram is also shown in Fig 6.

4.2 Numerical continuation of codimension-two bifurcation of E_3^*

Here we present codimension-two bifurcation numerically. We take $\beta = 4.8$ and vary a and c as bifurcation parameters. According to theorem 4, there is a 1:2 resonance point(R2) at $a = 8.0$ and $c = 1.2$, as shown in Fig. 7. The MATCONTM expression is given as
 label= R2, $x = (0.833333 \ 4.000000 \ 8.000000 \ 1.2000000)$.

The normal form coefficient(NFC) for R2 is: $[C,d] = -8.520711e-01, -1.704142e+00$.

According to theorems 4, 5 and 6, the system (4) undergoes 1:2, 1:3, and 1:4 resonance bifurcations at fixed point E_3^* . These resonance bifurcations, detected by R2, R3, and R4, are shown in Fig. 8. The MATCONTM gives
 label for R4, $x = (0.416667 \ 2.000000 \ 4.000000 \ 2.4000000)$
 NFC of R4: $A = -7.442084e-01$
 label for R3, $x = (0.6250000 \ 3.000000 \ 6.000000 \ 1.6000000)$
 NFC of R3: $\text{Re}(C_1) = -2.857143e-01$
 label for R2, $x = (0.833333 \ 4.000000 \ 8.000000 \ 1.2000000)$
 NFC for R2: $[C, d] = -8.520711e-01, -1.704142e+00$.

For the same set of parameters, the 1:2 resonance bifurcation diagram corresponding to Fig. 8 is shown in Fig. 9 at $c = 1.2$.

4.3 Orbits of period 3

We detect the closed region neighborhood of R3 by selecting the R3 point in Fig. 8, a closed invariant curve seems that

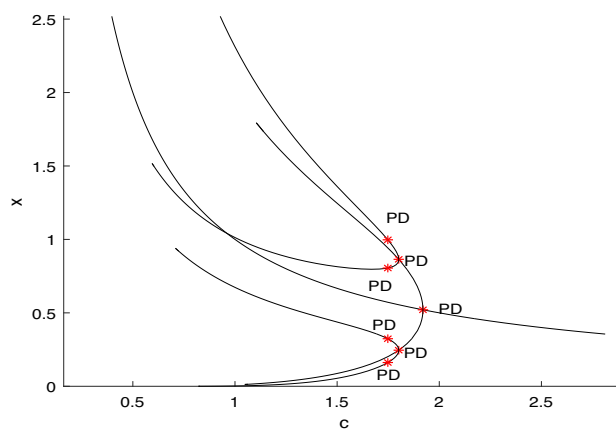


Fig. 5 Cascade of PD-points 2-cycles and 4-cycles

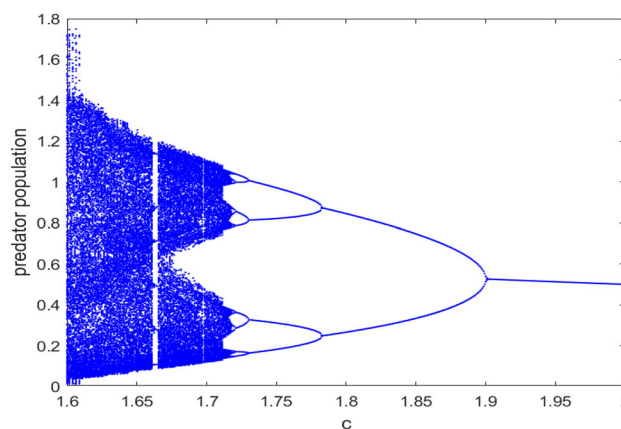


Fig. 6 Period-doubling bifurcation diagram with respect to c corresponding to fig 5

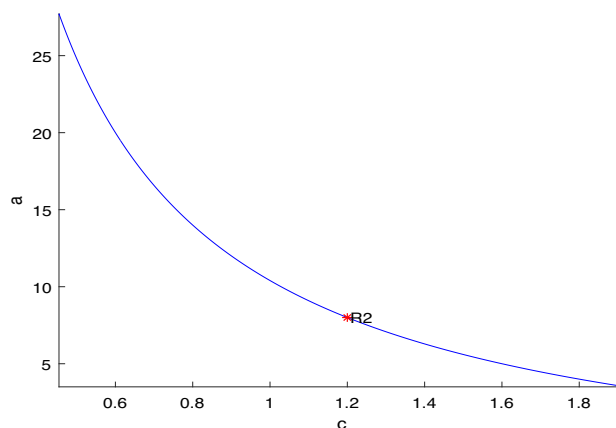


Fig. 7 1:2 resonance point detect by R2 emanating from PD point

coexists with an unstable fixed point i.e. the Neimark–Sacker curve, rooted at R3 in the third iteration, is drawn in Fig. 10. The 1:4 resonance bifurcation diagram is plotted in Fig. 11 corresponding to Fig. 8. The resonance 1:4 indicates that at the unique fixed point E_3^* , the closed invariant curve loses its

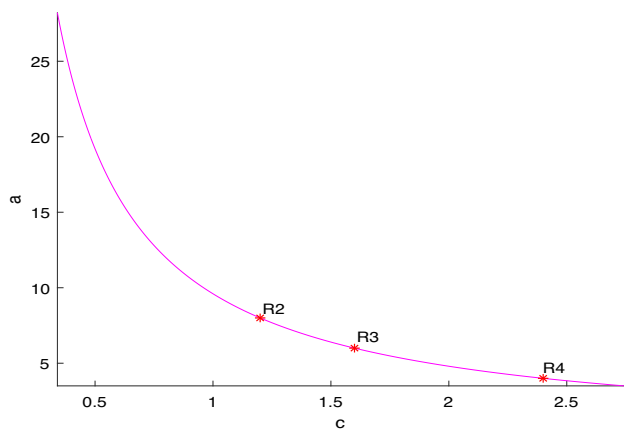


Fig. 8 Neimark–Sacker bifurcation including curve of 1:2 resonance (R2), 1:3 resonance (R3), 1:4 resonance (R4) in (c, a) -space

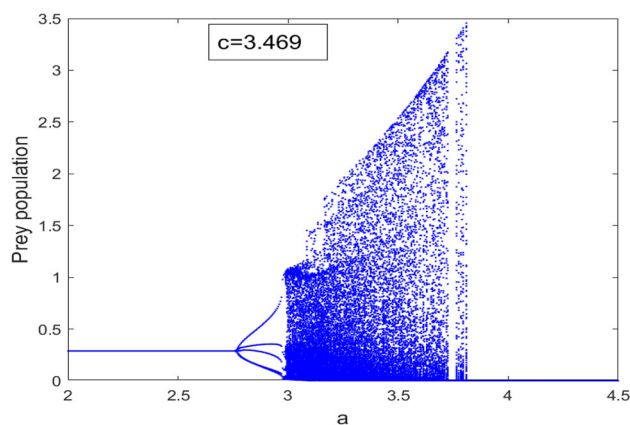


Fig. 11 1:4 Resonance bifurcation diagram

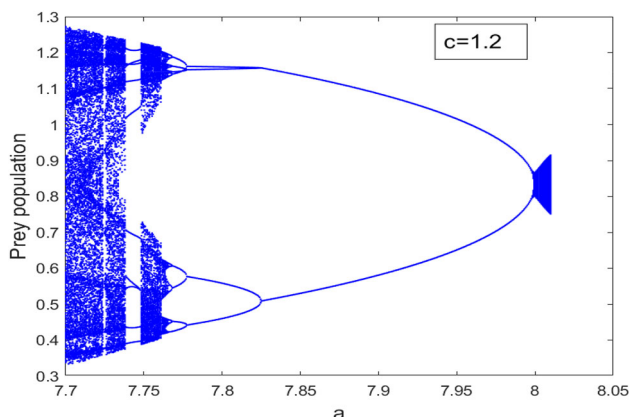


Fig. 9 1:2 Resonance bifurcation diagram

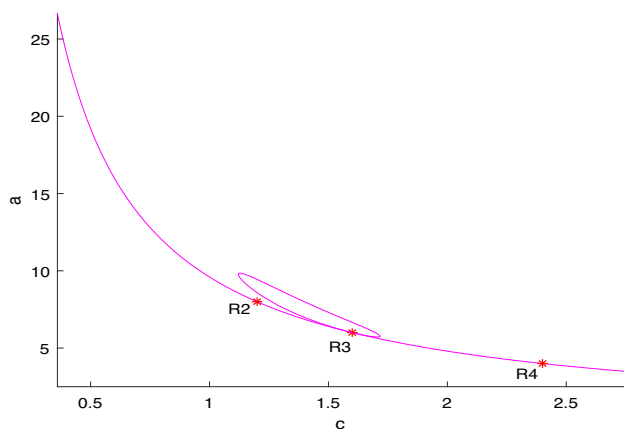


Fig. 10 Neimark–Sacker curve of third iteration rooted at R3 bifurcation point in (c, a) -space

smoothness and destroys when the saddle cycle of period-4 appears. The trajectory goes to period 4 orbits followed by chaos.

4.4 Biological interpretation

We studied the complex dynamical behavior of two species discrete-time model (4), in which, the existence and local stability of all fixed points are discussed. The map undergoes codim-1 bifurcation viz., fold bifurcation, flip bifurcation and Neimark–Sacker bifurcation at positive fixed point. These bifurcations mean both species (prey–predator) coexist in the neighborhood of an interior fixed point. Further, we obtained strong resonance bifurcation R2, R3, and R4 at a coexistence fixed point.

Biologically, the occurrence of R2 resonance bifurcation occurs at E_3^* implies that the discrete model may exhibit Neimark–Sacker, pitchfork, and heteroclinic bifurcation in the neighborhood of fixed points. The 1:3 resonance bifurcation reveals that an invariant curve of period three is bifurcated from the fixed point.

Moreover, the R4 resonance bifurcation demonstrates that both prey and predator coexist till order 4 in stable periodic cycles in the neighborhood of some critical parametric values.

Resonance bifurcation reveals the existence of multiple stable high periodic cycles between prey and predator in the ecosystem. Also, it furnishes a variety of strategies for the long-term coexistence of both species.

5 Conclusion

The two-dimensional continuous-time models show local and global behavior including limit cycles [56–58]. A difference equation describes interactions among non-overlapping generations. In this paper, we investigated a predator–prey discrete-time system with a linear functional response. We obtained our discretized model by deploying the piecewise constant argument approach and discussed the local stability around each fixed point. The bifurcations of codimension

one and codimension two in the map (4) by using the critical normal form coefficient technique are investigated. The codimension one bifurcation including flip(period-doubling) bifurcation, fold bifurcation and Neimark–Sacker bifurcation (NSB) and codim-2 bifurcations viz. 1:2 resonance, 1:3 resonance and resonance 1:4 are determined. The numerical continuation confirms the dynamics of the system around the fixed point. The occurrence of different types of bifurcations indicates the dynamical behavior of the discrete systems with various complexity from different characteristics. The complex dynamical behavior could be helpful to understand the dynamics of interactive predator and prey systems. For illustration, the appearance of a fold bifurcation implies that a fixed point must exist for all values of a parameter and can never be destroyed i.e. the fixed point may change its stability on varying parametric values. Moreover, the occurrence of flip bifurcation is not desirable in prey-predator models as it may induce a risk of extinction of either prey or predator species. The period-doubling bifurcation indicates that the discrete-time system will vary from a fixed point to a period-2 cycle when the parameter varies. i.e both species (prey and predator) may coexist in period-2 cycles under some conditions. The Neimark–Sacker bifurcation reveals that the dynamic changes from a stable fixed point to attracting cycles including periodic windows and chaotic attractors. Biologically speaking, NSB signifies that both species can fluctuate near critical parameter value and stable fluctuations seem. If $c_{NS} < 0$ then it will certainly continue.

The model may exhibit flip bifurcation, Neimark–Sacker bifurcation and hetroclinic bifurcation near 1:2 resonance point. The 1:3 resonance bifurcation indicates that an invariant curve of period three is bifurcated from the fixed point.

Moreover, the 1:4 resonance bifurcation demonstrates that both species coexist till order 4 in stable periodic cycles near some critical parametric values. Ecologically, the prey-predator system coexists up to the fourth order in the stable high periodic cycle. The prey and predator population can produce their density and survive mutually. On the invariant curve, the behavior of the fixed point can be quasi-periodic or periodic. However, the investigation of higher codimension bifurcations and chaos control are yet interesting problems. They may be assessed in future studies.

Acknowledgements The authors thank the Editor and anonymous Reviewers for handling this article and providing their helpful comments which significantly improved the scientific contents of the work.

Author Contributions V.S.S. contributed to conceptualization, visualization, software, resources, formal analysis, investigation, and writing—original draft. A.S. performed investigation, supervision, formal analysis, and writing—review and editing. A.E. performed investigation, formal analysis, and writing—review and editing. A.A.E. contributed to conceptualization, visualization, formal analysis, investigation, resources, visualization, and writing—review and editing.

Funding This study is supported by Core Research Grant, Science Engineering Research Board, Govt. of India (CRG/2021/006380). The work of Vijay Shankar Sharma is supported by the University Grant Commission (UGC), Govt. of India. This study is also supported via funding from Prince Sattam bin Abdulaziz University project number (PASU/2023/R/1444).

Data availability The data used in this research are available/mentioned within the manuscript.

Declarations

Conflict of interest The authors declare that they have no conflict of interest.

References

1. Lotka AJ (1925) Elements of physical biology. Williams & Wilkins
2. Volterra V (1928) Variations and fluctuations in the number of individuals in cohabiting animal species
3. Du Y, Peng R, Wang M (2009) Effect of a protection zone in the diffusive Leslie predator-prey model. *J Differ Equ* 246(10):3932–3956
4. Gakkhar S, Singh A (2012) Control of chaos due to additional predator in the hastings-powell food chain model. *J Math Anal Appl* 385(1):423–438
5. Huang J-C, Xiao D-M (2004) Analyses of bifurcations and stability in a predator-prey system with holling type-iv functional response. *Acta Math Appl Sin* 20(1):167–178
6. Huang J, Gong Y, Ruan S (2013) Bifurcation analysis in a predator-prey model with constant-yield predator harvesting. *Discret Contin Dyn Syst-B* 18(8):2101
7. Din Q (2017) Complexity and chaos control in a discrete-time prey-predator model. *Commun Nonlinear Sci Numer Simul* 49:113–134
8. Khan A (2016) Neimark-sacker bifurcation of a two-dimensional discrete-time predator-prey model. *Springerplus* 5(1):1–10
9. Singh A, Deolia P (2021) Bifurcation and chaos in a discrete predator-prey model with holling type-iii functional response and harvesting effect. *J Biol Syst* 1:1–28
10. Wang J, Cheng H, Liu H, Wang Y (2018) Periodic solution and control optimization of a prey-predator model with two types of harvesting. *Adv Differ Equ* 2018(1):1–14
11. Xiao D, Ruan S (2001) Global analysis in a predator-prey system with nonmonotonic functional response. *SIAM J Appl Math* 61(4):1445–1472
12. Liu B, Teng Z, Chen L (2006) Analysis of a predator-prey model with holling ii functional response concerning impulsive control strategy. *J Comput Appl Math* 193(1):347–362
13. Elabbasy E, Elsadany A, Zhang Y (2014) Bifurcation analysis and chaos in a discrete reduced lorenz system. *Appl Math Comput* 228:184–194
14. Singh A, Elsadany AA, Elsonbaty A (2019) Complex dynamics of a discrete fractional-order Leslie–Gower predator-prey model. *Math Methods Appl Sci* 42(11):3992–4007
15. Cheng L, Cao H (2016) Bifurcation analysis of a discrete-time ratio-dependent predator-prey model with Allee effect. *Commun Nonlinear Sci Numer Simul* 38:288–302
16. He Z, Lai X (2011) Bifurcation and chaotic behavior of a discrete-time predator-prey system. *Nonlinear Anal Real World Appl* 12(1):403–417
17. Jing Z, Yang J (2006) Bifurcation and chaos in discrete-time predator-prey system. *Chaos Solitons Fract* 27(1):259–277

18. Huang J, Liu S, Ruan S, Xiao D (2018) Bifurcations in a discrete predator-prey model with nonmonotonic functional response. *J Math Anal Appl* 464(1):201–230
19. Din Q (2013) Dynamics of a discrete Lotka–Volterra model. *Adv Differ Equ* 2013(1):1–13
20. Li L, Wang Z-J (2013) Global stability of periodic solutions for a discrete predator-prey system with functional response. *Nonlinear Dyn* 72(3):507–516
21. Liu W, Cai D (2019) Bifurcation, chaos analysis and control in a discrete-time predator-prey system. *Adv Differ Equ* 2019(1):1–22
22. Hu Z, Teng Z, Zhang L (2011) Stability and bifurcation analysis of a discrete predator-prey model with nonmonotonic functional response. *Nonlinear Anal Real World Appl* 12(4):2356–2377
23. Fan M, Wang K (2002) Periodic solutions of a discrete time nonautonomous ratio-dependent predator-prey system. *Math Comput Model* 35(9–10):951–961
24. Din Q (2018) Controlling chaos in a discrete-time prey-predator model with allee effects. *Int J Dyn Control* 6(2):858–872
25. Hogarth W, Norbury J, Cunning I, Sommers K (1992) Stability of a predator-prey model with harvesting. *Ecol Model* 62(1–3):83–106
26. Smith JM (1968) *Mathematical ideas in biology*. CUP Archive
27. Levine SH (1975) Discrete time modeling of ecosystems with applications in environmental enrichment. *Math Biosci* 24(3–4):307–317
28. Liu X, Xiao D (2006) Bifurcations in a discrete time Lotka–Volterra predator-prey system. *Discret Contin Dyn Syst-B* 6(3):559
29. Hadelor K, Gerstmann I (1990) The discrete Rosenzweig model. *Math Biosci* 98(1):49–72
30. Li S, Zhang W (2010) Bifurcations of a discrete prey-predator model with holling type ii functional response. *Discret Contin Dyn Syst-B* 14(1):159
31. Agiza H, Elabbasy E, El-Metwally H, Elsadany A (2009) Chaotic dynamics of a discrete prey-predator model with holling type ii. *Nonlinear Anal Real World Appl* 10(1):116–129
32. Singh A, Deolia P (2020) Dynamical analysis and chaos control in discrete-time prey-predator model. *Commun Nonlinear Sci Numer Simul* 90:105313
33. Murakami K (2007) Stability and bifurcation in a discrete-time predator-prey model. *J Differ Equ Appl* 13(10):911–925
34. Yuan L-G, Yang Q-G (2015) Bifurcation, invariant curve and hybrid control in a discrete-time predator-prey system. *Appl Math Model* 39(8):2345–2362
35. Xiao D, Li W, Han M (2006) Dynamics in a ratio-dependent predator-prey model with predator harvesting. *J Math Anal Appl* 324(1):14–29
36. Elsadany A, Din Q, Salman S (2020) Qualitative properties and bifurcations of discrete-time bazykin-berezovskaya predator-prey model. *Int J Biomath* 13(06):2050040
37. Elaydi SN (2007) *Discrete chaos: with applications in science and engineering*. Chapman and Hall/CRC
38. Elabbasy E, Agiza H, El-Metwally H, Elsadany A (2007) Bifurcation analysis, chaos and control in the burgers mapping. *Int J Nonlinear Sci* 4(3):171–185
39. Kuznetsov YA (1998) Elements of applied bifurcation theory. *Appl Math Sci* 112:591
40. Kuznetsov YA, Meijer HG (2005) Numerical normal forms for codim 2 bifurcations of fixed points with at most two critical eigenvalues. *SIAM J Sci Comput* 26(6):1932–1954
41. Alidousti J, Eskandari Z, Fardi M, Asadipour M (2021) Codimension two bifurcations of discrete Bonhoeffer-van der Pol oscillator model. *Soft Comput* 25(7):5261–5276
42. Eskandari Z, Alidousti J (2020) Stability and codimension 2 bifurcations of a discrete time sir model. *J Frankl Inst* 357(15):10937–10959
43. Eskandari Z, Alidousti J (2021) Generalized flip and strong resonances bifurcations of a predator-prey model. *Int J Dyn Control* 9:275–287
44. Ghaziani RK, Govaerts W, Sonck C (2012) Resonance and bifurcation in a discrete-time predator-prey system with holling functional response. *Nonlinear Anal Real World Appl* 13(3):1451–1465
45. Naik PA, Eskandari Z, Shahraki HE (2021) Flip and generalized flip bifurcations of a two-dimensional discrete-time chemical model. *Math Model Numer Simul Appl* 1(2):95–101
46. Eskandari Z, Avazzadeh Z, Ghaziani RK (2023) Theoretical and numerical bifurcation analysis of a predator-prey system with ratio-dependence. *Math Sci* 1:1–12
47. Naik PA, Eskandari Z, Yavuz M, Zu J (2022) Complex dynamics of a discrete-time Bazykin–Berezovskaya prey-predator model with a strong Allee effect. *J Comput Appl Math* 413:114401
48. Naik PA, Eskandari Z, Avazzadeh Z, Zu J (2022) Multiple bifurcations of a discrete-time prey-predator model with mixed functional response. *Int J Bifurc Chaos* 32(04):2250050
49. Huiwang G, Hao W, Wenxin S, Xuemei Z (2000) Functions used in biological models and their influences on simulations
50. Holling CS (1965) The functional response of predators to prey density and its role in mimicry and population regulation. *Memoirs Entomol Soc Canada* 97(S45):5–60
51. Elsadany A, Matouk A (2015) Dynamical behaviors of fractional-order Lotka–Volterra predator-prey model and its discretization. *J Appl Math Comput* 49(1):269–283
52. Din Q (2019) Stability, bifurcation analysis and chaos control for a predator-prey system. *J Vib Control* 25(3):612–626
53. Lin Y, Din Q, Rafaqat M, Elsadany AA, Zeng Y (2020) Dynamics and chaos control for a discrete-time Lotka–Volterra model. *IEEE Access* 8:126760–126775
54. Govaerts W, Ghaziani RK, Kuznetsov YA, Meijer HG (2007) Numerical methods for two-parameter local bifurcation analysis of maps. *SIAM J Sci Comput* 29(6):2644–2667
55. Kuznetsov IA, Meijer HGE (2019) *Numerical Bifurcation Analysis of Maps: From Theory to Software*. Cambridge University Press, Cambridge
56. May RM, Oster GF (1976) Bifurcations and dynamic complexity in simple ecological models. *Am Nat* 110(974):573–599
57. Sáez E, González-Olivares E (1999) Dynamics of a predator-prey model. *SIAM J Appl Math* 59(5):1867–1878
58. Liz E (2007) Local stability implies global stability in some one-dimensional discrete single-species models. *Discret Contin Dyn Syst-B* 7(1):191

Springer Nature or its licensor (e.g. a society or other partner) holds exclusive rights to this article under a publishing agreement with the author(s) or other rightsholder(s); author self-archiving of the accepted manuscript version of this article is solely governed by the terms of such publishing agreement and applicable law.